4. RECENT GUIDELINES FOR DESIGN AND OPTIMISATION OF AXIAL FLOW TURBOMACHINERY

4.1. Rotor blade circulation distribution along the radius

The total pressure rise performed by the blading at a given radius is as follows:

$$\Delta p_t = \eta_h \Delta p_{tid} = p_{2t} - p_{1t} \tag{4.1}$$

Where the total pressure upstream of the rotor is

$$p_{1t} = p_1 + \frac{\rho}{2} c_1^2 = const \tag{4.2}$$

Can be considered as constant along the radius. With neglect of losses upstream of the rotor, for example, having a rotor sucking from the surroundings, the upstream total pressure is equal to the atmospheric pressure.

The total pressure downstream of the rotor is

$$p_{2t} = p_2 + \frac{\rho}{2} c_2^2 \tag{4.3}$$

Which is not necessarily constant along the radius. Its distribution is depends on the design concept.

Let us consider the following:

$$\frac{dp_2}{dr} = \rho \frac{\Delta c_u^2}{r} \tag{4.4a}$$

According to the normal component equation of the Euler equation, expressed in the natural coordinate system [3].

Furthermore,

$$c_2^2 = c_{2a}^2 + \Delta c_u^2 \tag{4.4b}$$

Neglecting the radial velocity component. It is also assumed that

$$\eta_h \approx const \tag{4.4c}$$

The hydraulic efficiency is assumed to be constant along the radius.

Let us derivate Eq. (4.3) with respect to the radius. The result, taking into consideration relationships (4.4), is as follows:

$$\eta_h \frac{d\left(\Delta p_{tid}\right)}{dr} = \rho \frac{\Delta c_u^2}{r} + \frac{\rho}{2} \frac{d}{dr}\left(c_{2a}^2 + \Delta c_u^2\right) = \rho \frac{\Delta c_u^2}{r} + \frac{\rho}{2} 2 c_{2a} \frac{dc_{2a}}{dr} + \frac{\rho}{2} 2 \Delta c_u \frac{d\left(\Delta c_u\right)}{dr} \tag{4.5}$$

In which

$$\rho \frac{\Delta c_u^2}{r} + \frac{\rho}{2} 2 \Delta c_u \frac{d\left(\Delta c_u\right)}{dr} = \rho \frac{\Delta c_u}{r}\left(\Delta c_u + r \frac{d\left(\Delta c_u\right)}{dr}\right) = \rho \frac{\Delta c_u}{r} \frac{d}{dr}\left(r\, \Delta c_u\right) \tag{4.6}$$

Therefore, Eq. (4.5) can be written as follows:

$$\eta_h \frac{d(\Delta p_{tid})}{dr} = \rho \frac{\Delta c_u}{r} \frac{d}{dr}\left(r\, \Delta c_u\right) + \rho\, c_{2a} \frac{dc_{2a}}{dr} \tag{4.7}$$

In the first term of the right-hand side, the derivative is to be extended by $\rho \frac{u}{r}$. Therefore, the quantity to be derivated will be the ideal total pressure rise, according to the Euler equation of turbomachines:

$$\eta_h \frac{d(\Delta p_{tid})}{dr} = \frac{\Delta p_{tid}}{\rho u^2} \frac{d(\Delta p_{tid})}{dr} + \rho\, c_{2a} \frac{dc_{2a}}{dr} \tag{4.8}$$

After rearrangement:

$$\frac{d(\Delta p_{tid})}{dr}\left[\eta_h - \frac{\Delta p_{tid}}{\rho u^2}\right] = \rho\, c_{2a} \frac{dc_{2a}}{dr} \tag{4.9}$$

Eq. (4.9) shows the relationship between the radial variance of the flow characteristics. It gives an aid to point out how the design radial distribution of ideal total pressure rise influences the distribution of the axial velocity.

According to **Fig. 4.1**, a linear relationship exists between the ideal pressure rise and the circulation around a blade element. Let us surround a blade element with a curve "g", consisting of tangential sections of length of blade pitch t, and two periodic streamlines. Expressing the circulation on this curve, with consideration that the line integrals eliminate each other on the periodic streamlines, the result is as follows:

$$\Gamma = \oint_g \underline{w}\, d\underline{s} = t\left(w_{1u} - w_{2u}\right) = t\, \Delta c_u = \frac{2r\pi}{N} \Delta c_u = \frac{2r\pi}{N\rho u} \rho\, u\, \Delta c_u = \frac{2\pi}{N\rho\omega} \Delta p_{tid} \tag{4.10}$$

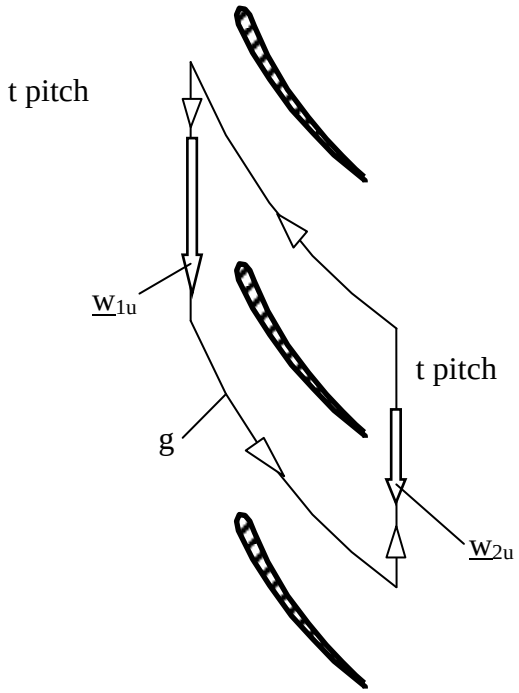

Fig. 4.1. Sketch for blade circulation

4.1.1. Design for spanwise constant ideal total pressure rise (I.E. FOR SPANWISE CONSTANT BLADE CIRCULATION) (Free vortex design)

Classic design method.

Substituting the condition of spanwise constant total pressure rise into Eq. (4.9) reads:

$$\frac{d\left(\Delta p_{tid}\right)}{dr}=0\Rightarrow \rho\, c_{2a}\frac{dc_{2a}}{dr}=0\Rightarrow c_{2a}\left(r\right)=const \tag{4.11}$$

ADANTAGES:

- Easy mathematical treatment.
- The outlet axial velocity is nearly constant in the annulus (**Fig. 4.2**). By this means, the friction losses originating from the rearrangement of the axial velocity profile can be reduced.

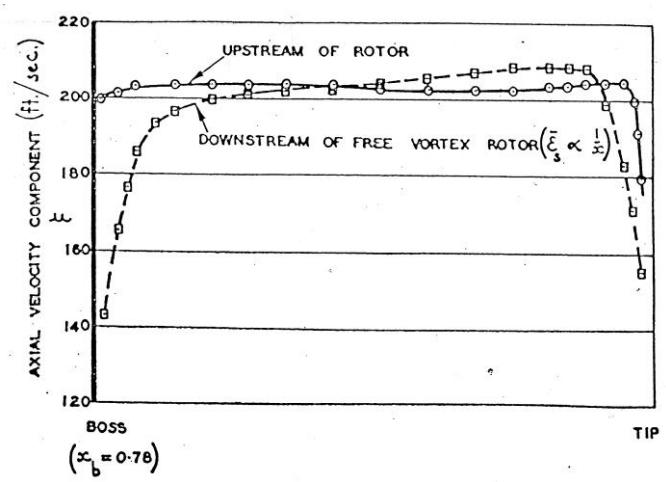

Fig. 4.2. Axial velocity profiles measured upstream and downstream of a free vortex rotor [10]

- Since the blade circulation is constant with radius, no vortices are shed from the trailing edge. As a result, the secondary losses can be minimised. The flow in the blade passage remains nearly 2D (no radial velocity), the measurement data on 2D airfoils and on linear cascades can be consequently used in design. **Fig. 4.3**.

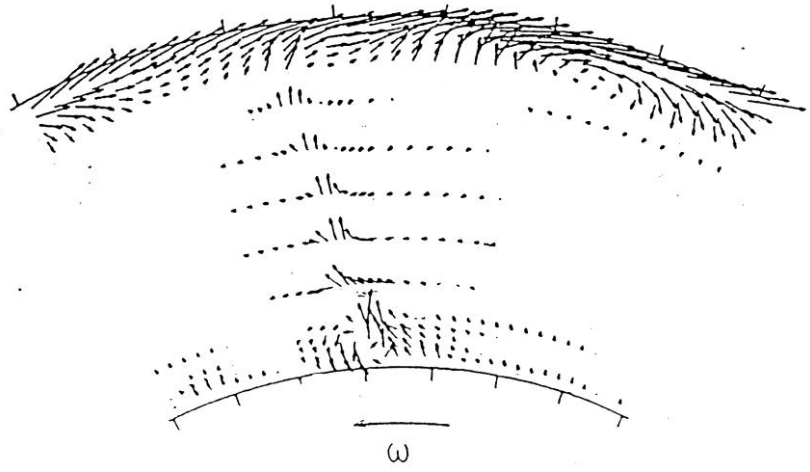

Fig. 4.3. Diagram of secondary flow measured downstream of a free vortex rotor [20]

LIMITS, DISADVANTAGES:

- Since

$$\Delta p_{tid}(r) = (\rho u\, \Delta c_u)(r) = const \qquad (4.12)$$

At the hub, where u is minimum, Δc_u must be maximum. This means that the maximum flow deflection is expected from the blading just at the hub, where the risk of flow separation is already increased due to flow friction on the hub and on the blade root. In order to avoid flow separation, the force factor $\frac{l}{t} c_f$ is to be limited at the hub in the design process. This limits the design Δp_{tid} at the hub, which is a limitation of the total pressure rise along the entire span, according to Eq. (4.12).

- Since u increases linearly along the span, Δc_u must decrease hyperbolically. Therefore, the blade sections at higher radius (moving at high circumferential speed) are less utilised.
- The above yield that only moderate specific performance, i.e. moderate Φ and Ψ can be realised by means of free vortex design.
- Since the axial velocity is constant along the span, but the circumferential velocity increases linearly with the radius, the velocity triangles "become stretched" with radius, the blade is twisted into the circumferential direction. Therefore, the blades are strongly twisted, and the chord length decreases with radius, according to the spanwise reduced load. The strong blade twist may cause complications in manufacturing.

4.1.2. Design for spanwise increasing ideal total pressure rise (I.E. FOR SPANWISE INCREASING BLADE CIRCULATION) (Controlled vortex design, non-free vortex design)

Modernised method, which meets the recent air technological demands for the high specific performance of a turbomachinery unit.

Lakshminarayana [4]: "the myth that the free-vortex blading has the lowest losses has been replaced by a more systematic optimisation".

(ON THE OTHER HAND: this discussion is related to the design point! The machine operates in accordance with the design concept at the design point only.)

Ideal total pressure rise increasing along the dominant part of span is prescribed.

The distributions must fulfil the following integral conditions:

The axial velocity distribution must correspond to the design volume flow rate:

$$q_V = \int_{d/2}^{D/2} c_{2a}(r) 2\pi r\, dr \qquad (4.13)$$

The axial velocity and ideal total pressure rise distributions must correspond to the design mean total pressure rise:

$$\overline{\Delta p_t} = \eta_h \frac{1}{q_V} \int_{d/2}^{D/2} \Delta p_{tid}(r) c_{2a}(r) 2\pi r\, dr \qquad (4.14)$$

ADVANTAGES:

- The fluid mechanical load at the blade root can be moderated in order to avoid flow separation at the hub.
- The blade section at higher radii are more loaded, the blading is more "utilised" along the entire span. This yields that the design specific performance can be increased.
- Blades of simplified geometry – i.e. of spanwise constant chord, or of moderate twist – can be designed. This may give simplifications in manufacturing.

LIMITS, DISADVANTAGES:

- More complicated mathematical treatment ⇔ design software! Although various design styles exist (e.g. exponential design [4], linear circulation distribution, etc.), an in-house developed design software makes possible the prescription of ARBITRARY circulation distribution. **Fig. 4.4**.

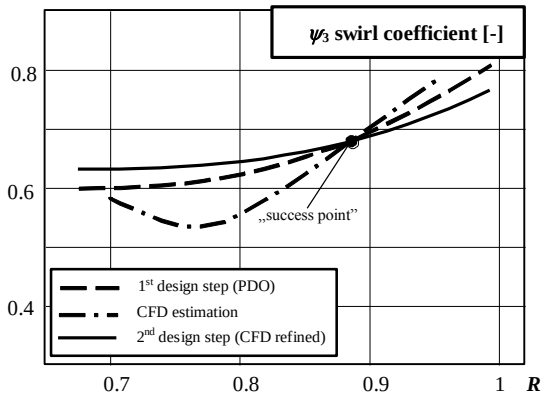

Fig. 4.4. Design blade circulation distributions [19]

- According to Eq. (4.9)

$$\frac{d\left(\Delta p_{tid}\right)}{dr}\left[\eta_h - \frac{\Delta p_{tid}}{\rho u^2}\right] = \rho\, c_{2a}\frac{dc_{2a}}{dr} \qquad (4.9)$$

Spanwise increasing circulation results in spanwise increasing axial velocity (**Fig. 4.5**). This means that the axial velocity profile is rearranged inside the blade passage. Uniformisation of the velocity downstream of the turbomachine is done by fluid friction, i.e. the non-uniform axial velocity is a source of losses. ⇔ This loss source is usually not as crucial as others (e.g. tip clearance loss). Downstream of the rotor, where the annulus is extended to the duct cross-section, the losses are increased anyway.

In some applications, e.g. **fog cannons**, it is just an advantage that the axial velocity is higher near the circumference (more effective transport of water droplets).

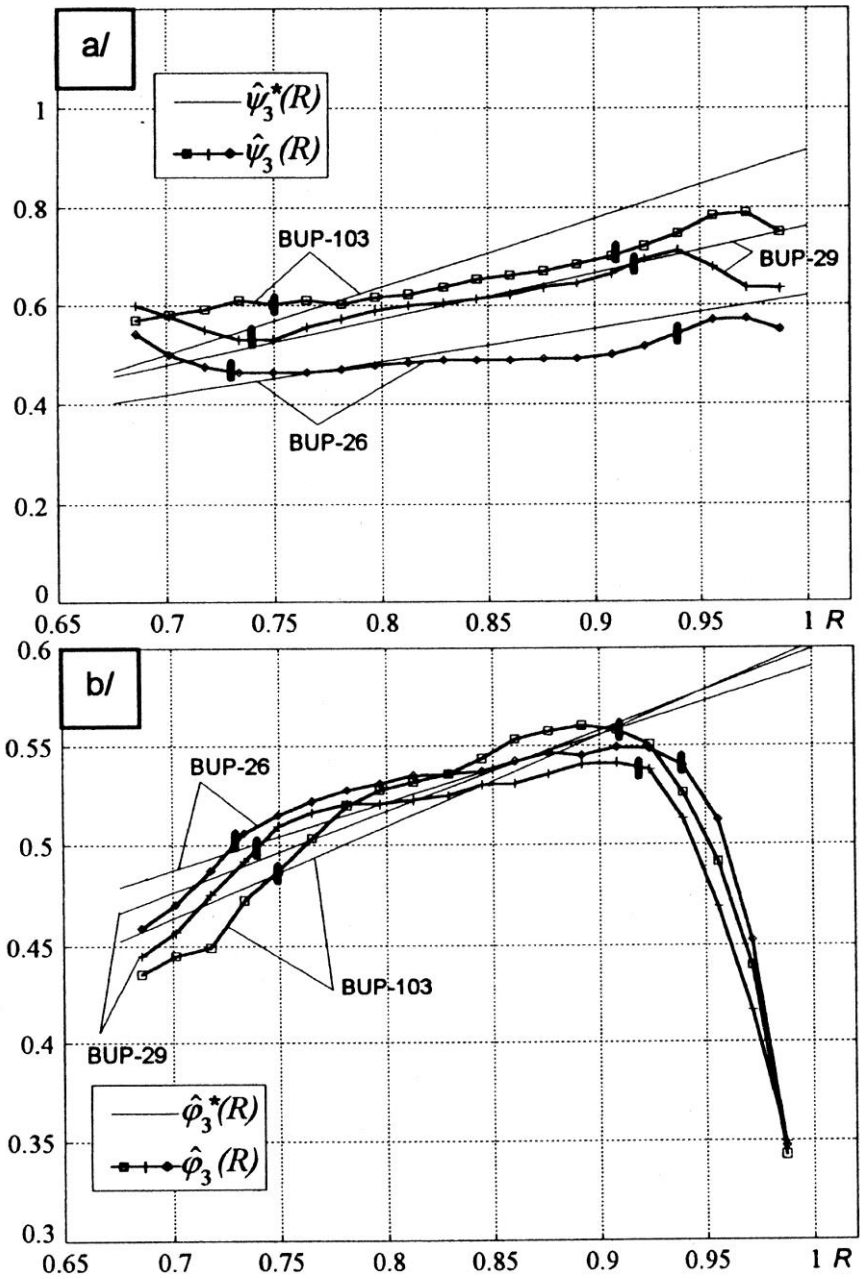

Fig. 4.5. Measured downstream axial velocity and ideal total pressure distributions [14]

- According to spanwise changing blade circulation, vortices are shed from the trailing edge, according to the Helmholtz 2nd law (**Fig. 4.6**). According to this law, a vortex tube cannot end in the flow field. It must either be closed to itself or must extend to the boundary of the flow domain. The increase of the blade circulation by dΓ, appearing as an additional vortex of circulation of dΓ, bounded in the blade, results in shedding of this vortex from the blade trailing edge. The shed vortices cause 3D flow in the blade passage, increasing the secondary losses (**Fig. 4.7**). The 3D flow features make the application of 2D airfoil or cascade data even more approximative. Such 3D effects can be considered in modern design by means of Computational Fluid Dynamics (CFD) simulation, e.g. with use of the software FLUENT.

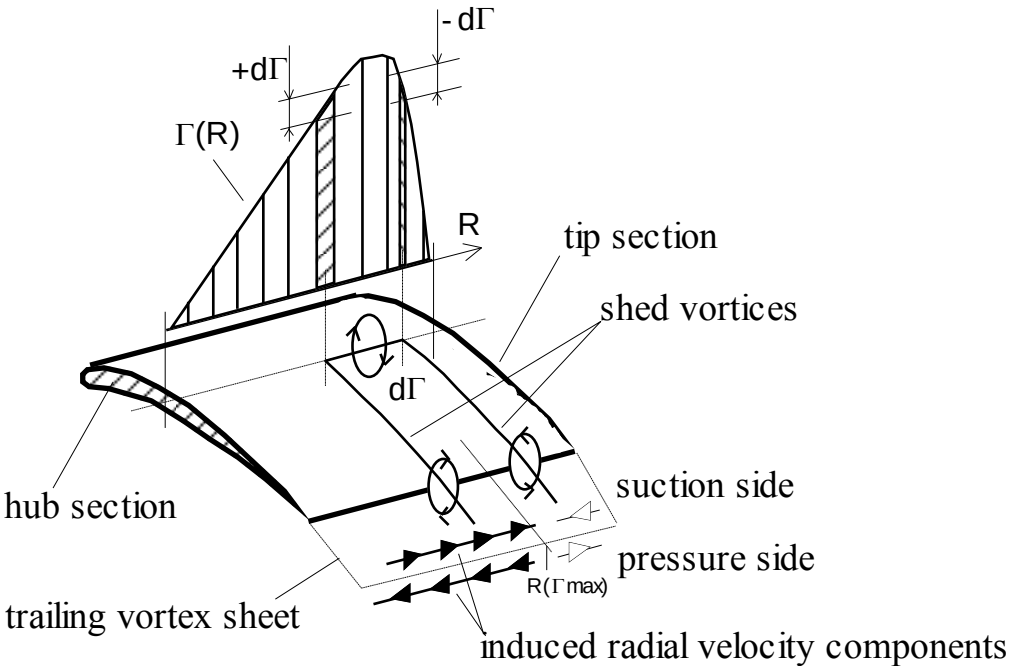

Fig. 4.6. Sketch of shed vorticity [22]

0.22 *X*:

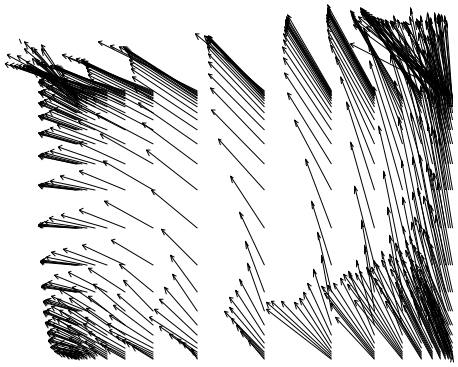

0.50 *X*:

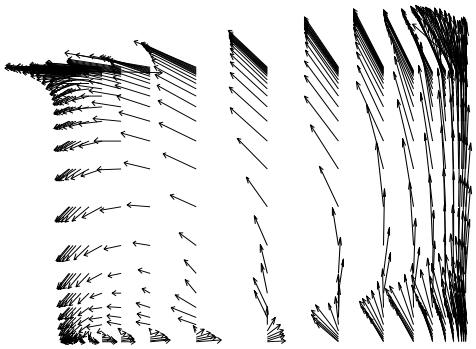

0.78 *X*:

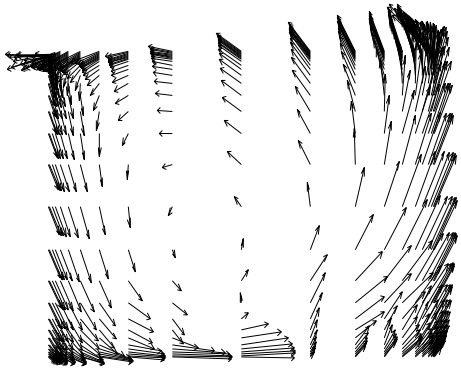

1.06 *X*:

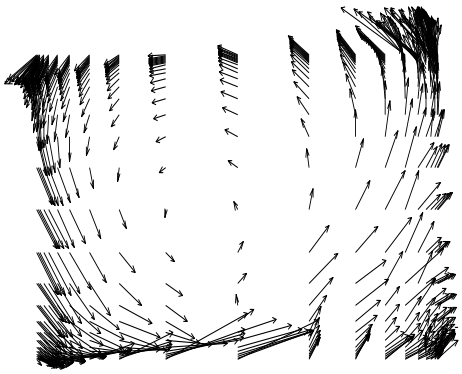

Fig. 4.7. Development of 3D flow in the blade passage. Secondary vector diagrams on planes normal to the axis of rotation. X: dimensionless axial coordinate. X = 0: leading edge. X = 1: trailing edge [23]

4.2. Blade stacking

4.2.1. Blade stacking techniques

Stacking line: the line connecting the centres of gravity of the blade sections at various radii. In the case of traditional blades, the stacking line is approximately a radial straight line ("straight blading"). The blades of modern axial flow machines – e.g. fans in air conditioning units, processor cooling fans, industrial compressors and gas turbines, compressors and gas turbines in airplane jet propulsion engines, etc. – often appear as blades of non-radial stacking.

In order to develop non-radial stacking, the following techniques can be applied, in analogy to the development of airplane wings (**Fig. 4.8**):

- Sweep: the blade section under consideration is shifted parallel to the relative flow direction. Sweep is often confined to the leading edge (see later). Sweep angle: λ .
- Dihedral (lean): the blade section under consideration is shifted normal to the relative flow direction. Dihedral angle: ν
- Skew: combination of the above.

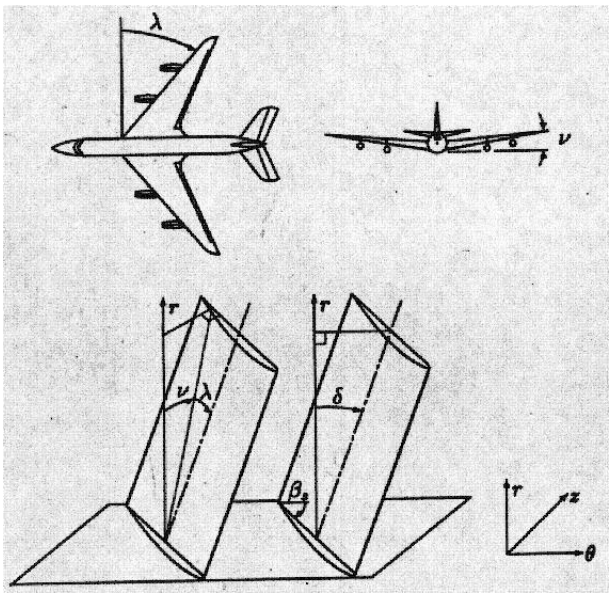

Fig. 4.8. Sweep, dihedral [24]

Further definitions:

- Positive sweep: the blade section under consideration is upstream of the adjacent inboard section. **Fig. 4.9.**
- Forward sweep: the blade section under consideration is upstream of the adjacent blade section at lower radius. **Fig. 4.10.**
- Positive lean: the endwall and the blade suction surface make an obtuse angle. **Fig. 4.11.**
- Circumferential forward skew: the stacking line is skewed in circumferential direction toward the direction of rotation. **Fig. 4.12.**

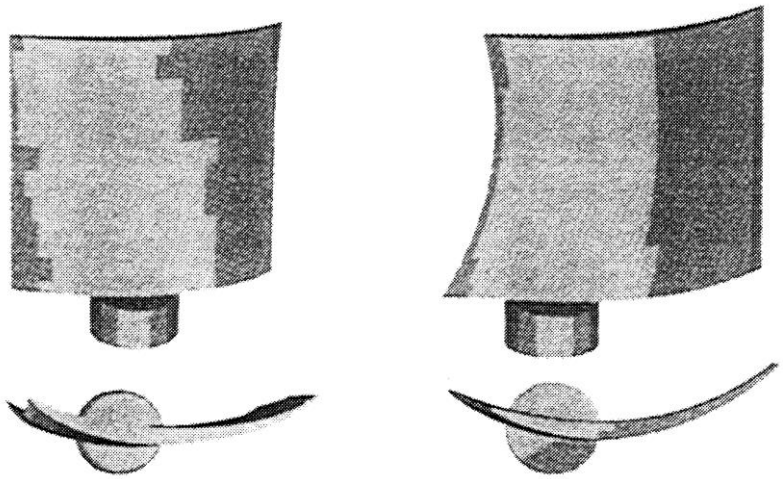

Fig. 4.9. Compressor blades with no sweep and with positive leading edge sweep at both blade ends [25]

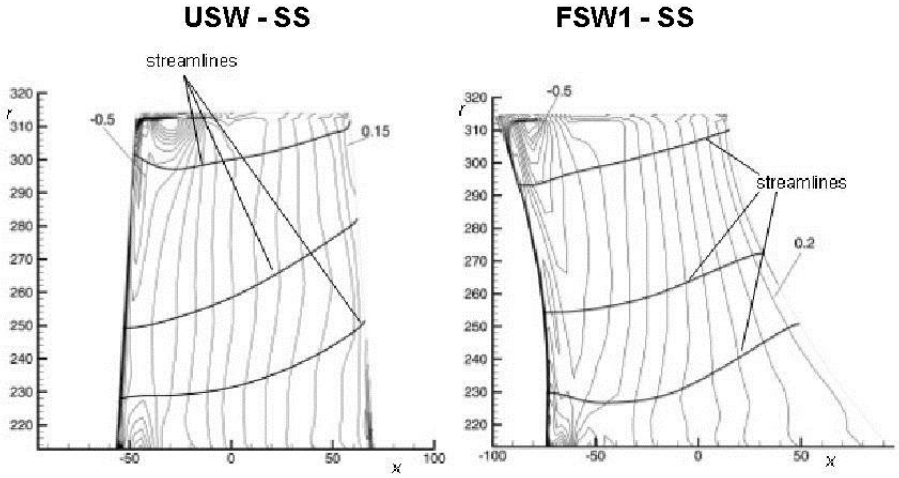

Fig. 4.10. Unswept and forward-swept rotor blading. CFD comparison [15]

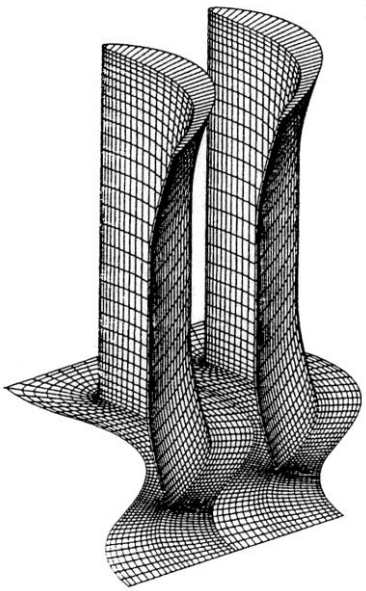

Fig. 4.11. Rotor blading with positive lean at both blade ends [26]

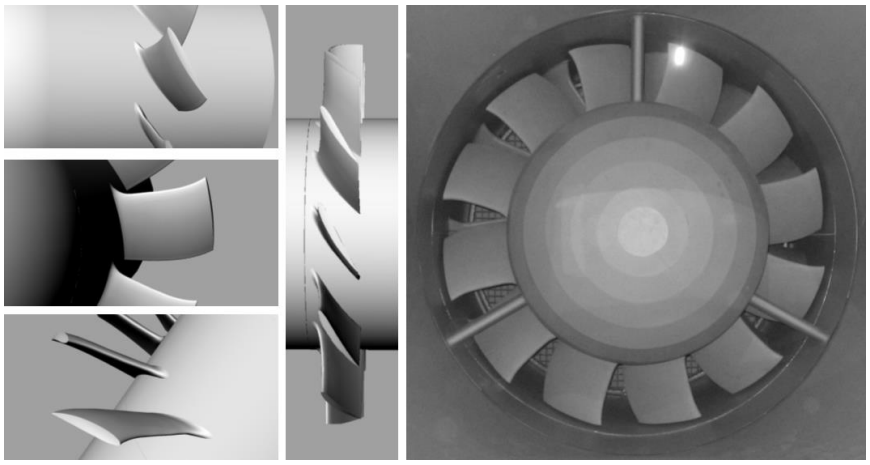

Fig. 4.12. Wind tunnel fan rotor with blades of circumferential forward skew, developed at the Department of Fluid Mechanics [27]

4.2.2. Advantageous effects

A/ Positive sweep and/or positive lean near the endwalls: loss reduction, efficiency improvement

- Reduces the load of the blade sections near the endwalls
- The blade load is shifted toward the trailing edge

By this means, the cross-passage pressure gradient between the pressure and suction sides is reduced. This results in

- Moderation of secondary flows
- Moderation of risk of separation at the endwall
- Moderation of tip clearance flow and the related losses

B/ Forward sweep: increased total pressure peak, extension of stall-free operating range

In the suction side boundary layer, the high loss fluid moves radially outward. This effect is more pronounced in throttled cases (flow rates lower than design). The high-loss fluid accumulates near the tip, making the flow conditions unfavourable in the entire blade passage. In an extreme case, the stagnating high-loss fluid blocks the entire blade passage and causes the breakdown of the characteristic curve (**stall margin**).

By sweeping the blades forward, the stagnating fluid can be evacuated from the blade passage. Therefore, the stall margin is shifted toward lower flow rate, and the maximum total pressure rise is also improved. **Fig. 4.13.**

The structural mechanical effects of non-radial stacking, e.g. forward sweep, are to be treated with strong criticism. For example, a forward-swept rotor blading has increased inclination to vibrate, and to deform due to the centrifugal forces.

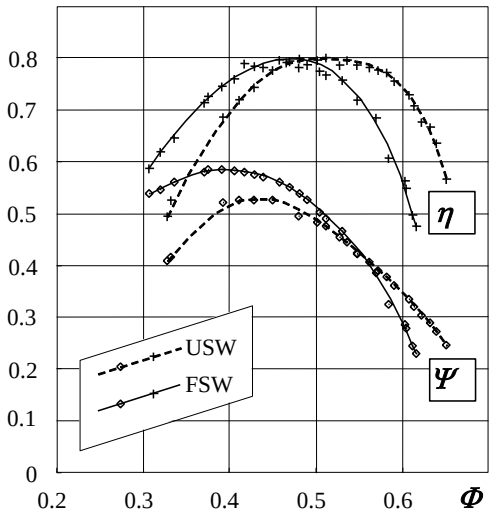

Fig. 4.13. Comparative characteristic curve measurements on fan rotors with unswept (USW) and forward-swept (FSW) blades [17]

C/ Sweep: reduction of shock losses

Shock losses develop in transonic compressors. On the suction side, the local velocity may reach the speed of sound, resulting in a shock. By means of sweep, the velocity component normal to the stacking line can be kept below the speed of sound, and therefore, the shock losses can be avoided.

D/ Sweep, circumferential skew: noise reduction

Due to the curved trailing edge, the noise caused by the interaction between the rotor blade and the elements downstream of it (e.g. OGV, motor support) can be reduced. This is because a temporarily more distributed interaction occurs instead of an impulse-like interaction. **Fig. 4.14**.

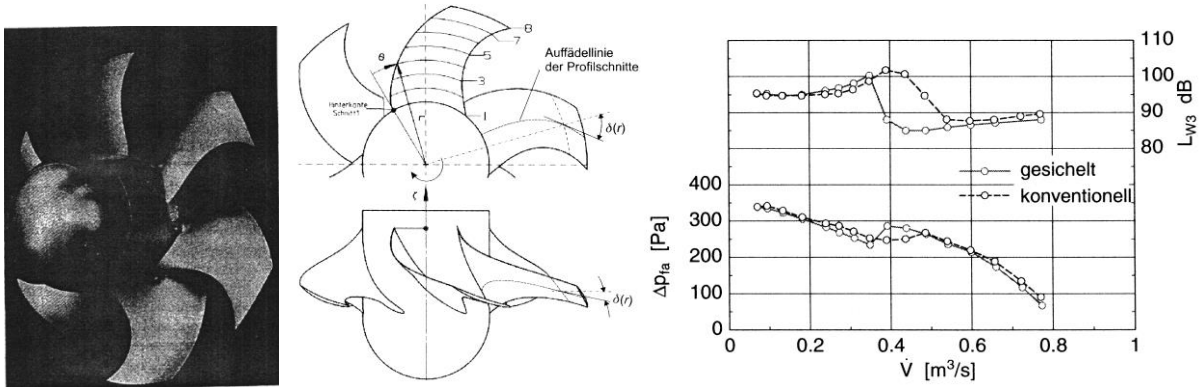

Fig. 4.14. Sickle-shaped („gesichelt", circumferentially forward skewed) rotor blading. Measured aerodynamic and acoustic characteristics: comparison with straight („ungesichelt") blading [24][28]